

Multiphilic Descriptor for Chemical Reactivity and Selectivity

J. Padmanabhan,^{†,‡,§} R. Parthasarathi,[‡] M. Elango,[‡] V. Subramanian,^{*,‡}
 B. S. Krishnamoorthy,^{†,§} S. Gutierrez-Oliva,[‡] A. Toro-Labbé,^{*,‡} D. R. Roy,[†] and
 P. K. Chattaraj^{*,†}

Department of Chemistry, Indian Institute of Technology, Kharagpur 721302, India, Chemical Laboratory, Central Leather Research Institute, Adyar, Chennai 600 020, India, School of Chemistry, Department of Physics, L. N. Government College, Ponneri 601 204, India, Bharathidasan University, Tiruchirappalli-620 024, India, and Laboratorio de Química Teórica Computacional (QTC), Facultad de Química, Pontificia Universidad Católica de Chile, Casilla 306, Correo 22, Santiago, Chile

Received: March 8, 2007; In Final Form: June 3, 2007

In line with the local philicity concept proposed by Chattaraj et al. (Chattaraj, P. K.; Maiti, B.; Sarkar, U. J. *J. Phys. Chem. A* **2003**, *107*, 4973) and a dual descriptor derived by Morell, Grand and Toro-Labbé, (*J. Phys. Chem. A* **2005**, *109*, 205), we propose a multiphilic descriptor. It is defined as the difference between nucleophilic (ω_k^+) and electrophilic (ω_k^-) condensed philicity functions. This descriptor is capable of simultaneously explaining the nucleophilicity and electrophilicity of the given atomic sites in the molecule. Variation of these quantities along the path of a soft reaction is also analyzed. Predictive ability of this descriptor has been successfully tested on the selected systems and reactions. Corresponding force profiles are also analyzed in some representative cases. Also, to study the intra- and intermolecular reactivities another related descriptor, namely, the nucleophilicity excess ($\Delta\omega_g^+$) for a nucleophile over the electrophilicity in it, has been defined and tested on all-metal aromatic compounds.

1. Introduction

The understanding of chemical reactivity and site selectivity of molecular systems has been effectively handled by the conceptual density functional theory (DFT).¹ Chemical potential, global hardness, global softness, electronegativity, and electrophilicity are global reactivity descriptors, highly successful in predicting global chemical reactivity trends. The Fukui function (FF) and local softness are extensively applied to probe the local reactivity and site selectivity. The formal definitions of all these descriptors and working equations for their computation have been described.^{1–4} Various applications of both global and local reactivity descriptors in the context of chemical reactivity and site selectivity have been reviewed in detail.³

Parr et al. introduced the concept of electrophilicity (ω) as a global reactivity index similar to the chemical hardness and chemical potential.⁵ This new reactivity index measures the stabilization in energy when the system acquires an additional electronic charge ΔN from the environment. The electrophilicity is defined as

$$\omega = \mu^2/2\eta \quad (1)$$

In eq 1, $\mu \approx -(I + A)/2$ and $\eta \approx (I - A)/2$ are the electronic chemical potential and the chemical hardness of the ground state of atoms and molecules, respectively, approximated in terms of the vertical ionization potential (I) and electron affinity (A).

* Authors to whom correspondence should be addressed. E-mail: subuchem@hotmail.com (V.S.); atola@puc.cl (A.T.-L.); pkc@chem.iitkgp.emet.in (P.K.C.).

[†] Indian Institute of Technology.

[‡] Central Leather Research Institute.

[§] L. N. Government College.

[§] Bharathidasan University.

[‡] Pontificia Universidad Católica de Chile.

The electrophilicity is a descriptor of reactivity that allows a quantitative classification of the global electrophilic nature of a molecule within a relative scale.⁵

The FF^{6–25} is one of the widely used local density functional descriptors^{6–25} to model chemical reactivity and site selectivity and is defined as the derivative of the electron density $\rho(\vec{r})$ with respect to the total number of electrons N in the system, at constant external potential $v(\vec{r})$ acting on an electron due to all the nuclei in the system

$$f(\vec{r}) = [\delta\mu/\delta v(\vec{r})]_N = [\partial\rho(\vec{r})/\partial N]_{v(\vec{r})} \quad (2)$$

The condensed-to-atom FFs are the Fukui indexes (FI) that are calculated using the procedure proposed by Yang and Mortier,⁷ based on a finite difference method:

$$f_k^+ = q_k(N + 1) - q_k(N) \quad \text{for nucleophilic attack} \quad (3a)$$

$$f_k^- = q_k(N) - q_k(N - 1) \quad \text{for electrophilic attack} \quad (3b)$$

$$f_k^0 = [q_k(N + 1) - q_k(N - 1)]/2 \quad \text{for radical attack} \quad (3c)$$

where q_k is the electronic population of atom k in a molecule.

Chattaraj et al.⁸ have introduced the concept of generalized philicity. It contains almost all information about the hitherto known different global and local reactivity and selectivity descriptors, in addition to the information regarding the electrophilic/nucleophilic power of a given atomic site in a molecule. It is possible to define a local quantity called philicity associated with a site k in a molecule with the help of the corresponding condensed-to-atom variants of FF, f_k^α as

$$\omega_k^\alpha = \omega f_k^\alpha \quad (4)$$

where $\alpha = +, -, \text{ and } 0$ represents the local philic quantities describing nucleophilic, electrophilic, and radical attacks, respectively. Equation 4 predicts that the most electrophilic site in a molecule is the one providing the maximum value of ω_k^+ . When two molecules react, which one will act as an electrophile (nucleophile) will depend on which has a higher (lower) electrophilicity index. This global trend originates from the local behavior of the molecules or precisely at the atomic site(s) that is (are) prone to electrophilic (nucleophilic) attack. Recently, the usefulness of the electrophilicity index in elucidating the toxicity of polychlorinated biphenyls, benzidine, and chlorophenol has been assessed in detail.^{9–11}

In addition to the knowledge of global softness (S), which is the inverse of hardness,¹² different local softnesses,¹³ used to describe the reactivity of atoms in molecule, can be defined as

$$s_k^\alpha = S f_k^\alpha \quad (5)$$

where $\alpha = +, -, \text{ and } 0$ represents local softness quantities describing nucleophilic, electrophilic, and radical attacks, respectively. On the basis of local softness, relative nucleophilicity (s_k^-/s_k^+) and relative electrophilicity (s_k^+/s_k^-) indices have also been defined, and their usefulness to predict reactive sites has also been addressed.¹⁴ Please note that the relative electro-(nucleo)philicity has no difference with the corresponding relative Fukui function.^{8b} It has been established that the quantum chemical model selected to derive the wave function, the population scheme used to obtain the partial charges, and the basis set employed in the molecular orbital calculations are important parameters, which significantly influence the FF and FI values.^{15–18}

The condensed philicity summed over a group of relevant atoms is defined as the “group philicity”. It can be expressed as¹⁹

$$\omega_g^\alpha = \sum_{k=1}^n \omega_k^\alpha \quad (6)$$

where n is the number of atoms coordinated to the reactive atom, ω_k^α is the local electrophilicity of the atom k , and ω_g^α is the group philicity obtained by adding the local philicity of the nearby bonded atoms. In this study¹⁹ the group nucleophilicity index (ω_g^+) of the selected systems is used to compare the chemical reactivity trends.

Toro-Labbé and co-workers^{20,23} have recently proposed a dual descriptor ($\Delta f(r)$), which is defined as the derivative of molecular hardness with respect to the external potential and can be expressed as the difference between the nucleophilic and electrophilic FFs, and is given by

$$\Delta f(r) = \left(\frac{\delta \eta}{\delta v(r)} \right)_N = \left(\frac{\partial f(r)}{\partial N} \right)_{v(r)} \cong [f^+(r) - f^-(r)] \quad (7)$$

If $\Delta f(r) > 0$, then the site is favored for a nucleophilic attack, whereas if $\Delta f(r) < 0$, then the site may be favored for an electrophilic attack. Following the above definition, the associated dual local softness have also been defined as the condensed version of $\Delta f(r)$ multiplied by the molecular softness S .¹⁹

$$\Delta s_k = S(f_k^+ - f_k^-) = (s_k^+ - s_k^-) \quad (8)$$

2. Multiphilic Descriptor

In the light of the local philicity⁸ and the dual descriptor^{20,23} we propose a multiphilic descriptor using the unified philicity

concept, which can concurrently characterize both the nucleophilic and electrophilic nature of a chemical species. It is defined as the difference between the nucleophilic and electrophilic condensed philicity functions. It is an index of selectivity toward nucleophilic attack, which can as well characterize an electrophilic attack, and is given by²¹

$$\Delta \omega_k = [\omega_k^+ - \omega_k^-] = \omega[\Delta f_k] \quad (9)$$

where Δf_k is the condensed-to-atom variant- k of $\Delta f(r)$ (eq 7). If $\Delta \omega_k > 0$, then the site k is favored for a nucleophilic attack, whereas if $\Delta \omega_k < 0$, then the site k may be favored for an electrophilic attack. Because FIs are positive, at least for the cases where relaxation and charge partitioning are properly taken care of, ($0 < f_k < 1$), $-1 < \Delta f_k < 1$, and the normalization condition for $\Delta \omega_k$ is

$$\sum_k \Delta \omega_k = \omega \sum_k \Delta f_k = 0 \quad (10)$$

Although $\Delta \omega_k$ and Δf_k will contain the same intramolecular reactivity information the former is expected to be a better intermolecular descriptor because of its global information content. Here ω takes care of the amount of electron transfer and f_k^α takes care of the direction of the same. Use of Δf_k provides the net electrophilicity (or net nucleophilicity) in terms of the net amount of electron transfer in a given direction. While dual local softness^{20,23} takes care of the hard–soft interactions at the local level, albeit with the possibility of ambiguity in the local hardness,²² $\Delta \omega_k$ is apt for the electrophile–nucleophile interactions.

We may analyze the nature of $\Delta \omega(\vec{r})$ in terms of that²² of $\Delta f(\vec{r})$ as follows:

$$\begin{aligned} \left(\frac{\partial \omega(\vec{r})}{\partial N} \right)_v &= \left(\frac{\partial [\omega f(\vec{r})]}{\partial N} \right)_v \\ &= \left(\frac{\partial \omega}{\partial N} \right)_v f(\vec{r}) + \omega \left(\frac{\partial f(\vec{r})}{\partial N} \right)_v \\ &= \left(\frac{\partial \omega}{\partial N} \right)_v f(\vec{r}) + \omega \Delta f(\vec{r}) \\ &= \left(\frac{\partial \omega}{\partial N} \right)_v f(\vec{r}) + \Delta \omega(\vec{r}) \\ \Delta \omega(\vec{r}) &= \left[\left(\frac{\partial \omega(\vec{r})}{\partial N} \right)_v - \left(\frac{\partial \omega}{\partial N} \right)_v f(\vec{r}) \right] \end{aligned}$$

The multiphilicity descriptor, $\Delta \omega(\vec{r})$ is a measure of the difference between local and global (modulated by $f(\vec{r})$) reactivity variations associated with the electron acceptance/removal. Incidentally, the variation of $(\partial \omega / \partial N)$ across the periodic table is similar to that of μ .²⁴

$$\begin{aligned} \left(\frac{\partial \omega}{\partial N} \right)_v &= \frac{\partial}{\partial N} \left[\frac{\mu^2}{2\eta} \right]_v \\ &= \frac{\mu(\partial \mu)}{\eta(\partial \eta)_v} - \frac{\mu^2}{4\eta^2} \left(\frac{\partial \eta}{\partial N} \right)_v \\ &= \frac{\mu}{\eta} \gamma - \frac{\mu^2}{4\eta^2} \gamma \\ &= \mu - \frac{\mu^2}{4\eta^2} \gamma = \mu - \frac{\omega \gamma}{2\eta} \end{aligned}$$

Since γ is generally very small,²⁵ $(\partial \omega / \partial N)_v$ is expected to follow the μ trend.

TABLE 1: Calculated Global Reactivity Properties of the Selected Molecules Using B3LYP/6-311+G and BLYP/DND Methods**

molecules	B3LYP/6-311+G** (eV)				BLYP/DND (eV)			
	η	μ	ω	S	η	μ	ω	S
HCHO	2.960	-4.707	3.742	0.169	1.942	-4.260	4.673	0.258
CH ₃ CHO	3.115	-4.224	2.864	0.161	2.096	-3.791	3.425	0.238
CH ₃ COCH ₃	3.144	-3.910	2.432	0.159	2.133	-3.456	2.800	0.234
C ₂ H ₅ COC ₂ H ₅	3.153	-3.799	2.288	0.159	2.151	-3.367	2.635	0.233
CH ₂ =CHCHO	2.503	-4.904	4.805	0.200	1.545	-4.413	6.303	0.324
CH ₃ CH=CHCHO	2.542	-4.631	4.217	0.197	1.593	-4.132	5.359	0.314
NH ₂ OH	3.869	-3.553	1.632	0.129	3.337	-2.513	0.946	0.150
CH ₃ ONH ₂	3.630	-3.738	1.925	0.138	3.377	-2.346	0.815	0.148
CH ₃ NHOH	3.482	-3.392	1.652	0.144	3.128	-2.284	0.833	0.160
OHCH ₂ CH ₂ NH ₂	3.343	-3.507	1.840	0.150	3.129	-2.125	0.722	0.160
CH ₃ SNH ₂	3.050	-3.331	1.819	0.164	2.258	-2.572	1.466	0.221
CH ₃ NHSH	3.148	-3.629	2.092	0.159	2.332	-2.998	1.928	0.214
SHCH ₂ CH ₂ NH ₂	3.135	-3.417	1.862	0.159	2.476	-2.586	1.351	0.202

Problems associated with the definition of η and the discontinuity²⁶ in E as a function of N will be present in the $\Delta f(\bar{r})$ definition and the discontinuity in $\rho(\bar{r})$. A similar type of differentiation has also been attempted by other research workers.²⁷ Also, to study the intra- and intermolecular reactivities another related descriptor, namely, nucleophilicity excess ($\Delta\omega_g^\mp$) for a nucleophile over the electrophilicity (net nucleophilicity) in it, is defined as

$$\Delta\omega_g^\mp = \omega_g^- - \omega_g^+ = \omega(f_g^- - f_g^+) \quad (11)$$

where $\omega_g^- (\equiv \sum_{k=1}^n \omega_k^-)$ and $\omega_g^+ (\equiv \sum_{k=1}^n \omega_k^+)$ are the group philicities of the nucleophile in the molecule due to electrophilic and nucleophilic attacks, respectively. It is expected that the nucleophilicity excess ($\Delta\omega_g^\mp$) for a nucleophile should always be positive, whereas it will provide a negative value for an electrophile in a molecule.

In the present study, we use both the multiphilicity descriptor and nucleophilicity excess to probe the nature of attack/reactivity at a particular site in the selected systems.

3. Computational Details

The geometries of HCHO, CH₃CHO, CH₃COCH₃, C₂H₅COC₂H₅, CH₂=CHCHO, CH₃CH=CHCHO, NH₂OH, CH₃ONH₂, CH₃NHOH, OHCH₂CH₂NH₂, CH₃SNH₂, CH₃NHSH, SHCH₂CH₂NH₂ are optimized by the B3LYP/6-311+G** level of theory and all-metal aromatic molecules, viz., MA₄⁻ (M = Li, Na, K, and Cu), by the B3LYP/6-311+G* method as available in the GAUSSIAN 98 package.²⁸ Various reactivity and selectivity descriptors such as chemical hardness, chemical potential, softness, electrophilicity, and the appropriate local quantities employing natural population analysis (NPA)^{29,30} scheme are calculated. The HPA scheme (Stockholder partitioning scheme)³¹ as implemented in the DMOL³ package³² has also been used to calculate the local quantities employing the BLYP/DND method. For all-metal aromatic molecules, the Δ SCF method has been utilized to compute the ionization potential (IP) and electron affinity (EA) according to the equations $I = E_{N-1} - E_N$, $A = E_N - E_{N+1}$, where IP and EA are obtained from total electronic energy calculations on the $N - 1$, N , $N + 1$ electron systems at the neutral molecule geometry.

4. Results and Discussion

A series of carbonyl compounds is selected in the present study to probe the usefulness of the multiphilicity descriptor

(Supporting Information Figure S1). A comparison with various other descriptors and the recently derived dual descriptor is also probed. Due to bipolar nature of the C=O bond, both nucleophilic and electrophilic attacks are possible at C and O sites. It is noted that the rate of nucleophilic addition on the carbonyl compound be reduced by electron-donating alkyl groups and enhanced by electron-withdrawing ones.³³ Recently, we have studied a set of these carbonyl compounds in the light of philicity and group philicity.¹⁹ The global molecular properties of the selected series of carbonyl compounds are presented in Table 1. Global electrophilicity trend for these molecules (toward a nucleophile) is as follows: CH₂=CHCHO > CH₃CH=CHCHO > HCHO > CH₃CHO > CH₃COCH₃ > C₂H₅COC₂H₅ (see Table 1). Various local quantities for particular sites of the selected systems are listed in Table 2. Selected compounds are grouped into two sets, namely, nonconjugated and α -, β -conjugated carbonyl compounds.

For the nonconjugated carbonyl compounds, the carbon atom (C₁) bearing the carbonyl group is expected to be the most reactive site toward a nucleophilic attack. Table 2 lists the values of local reactivity descriptors using the B3LYP/6-311+G** method for NPA-derived charges of the selected molecules. NPA-derived local quantities predict the expected maximum value for carbonyl carbon (C₁) of all the selected molecules for f_k^+ , s_k^+ , and ω_k^+ . But s_k^+/s_k^- is unable to provide the maximum value for the C₁ atom due to negative FI values. One important point to note is that among the descriptors f_k^+ , s_k^+ , ω_k^+ , and s_k^+/s_k^- , the ω_k^+ value is capable of providing a clear distinction between carbonyl carbon (C₁) and the oxygen site for nucleophilic attack.

Since HPA-derived charges generally provide non-negative FI³⁴ values, we also made use of it for local reactivity analysis on carbonyl compounds. HPA-derived local reactivity descriptors also predict the expected maximum value for the C₁ atom in the case of HCHO and CH₃CHO but fail to predict it for CH₃COCH₃ and C₂H₅COC₂H₅, where the oxygen atom is shown to be prone toward nucleophilic attack. Nevertheless, the f_k^+ value of oxygen is almost the same as that of the carbonyl carbon (C₁), thus making it difficult to make a clear decision on the electrophilic behavior of these atoms. Under these situations, dual descriptors $\Delta f(r)$, Δs_k , and multiphilicity descriptor $\Delta\omega(r)$, give a helping hand. All these quantities provide a clear difference between nucleophilic and electrophilic attacks at a particular site with their sign. That is, they provide a positive value for a site prone for nucleophilic attack and a negative value at the site prone for electrophilic attack. The advantage

TABLE 2: Calculated Local Reactivity Properties of the Selected Molecules Using NPA (B3LYP/6-311+G) and HPA (BLYP/DND) Derived Charges**

molecule			f_k^+	f_k^-	s_k^+	s_k^-	s_k^+/s_k^-	ω_k^+	ω_k^-	$\frac{\Delta f_k}{f_k^+ - f_k^-} =$	$\frac{\Delta s_k}{s_k^+ - s_k^-} =$	$\frac{\Delta \omega_k}{\omega_k^+ - \omega_k^-} =$
HCHO	C	NPA	0.8323	-0.1722	0.1407	-0.0291	-4.8333	3.1145	-0.6444	1.0045	0.1698	3.7588
		HPA	0.3973	0.2373	0.1025	0.0612	1.6743	1.8566	1.1089	0.1600	0.0413	0.7477
	O	NPA	0.0399	0.9409	0.0067	0.1590	0.0424	0.1493	3.5208	-0.9010	-0.1523	-3.3715
		HPA	0.3010	0.4232	0.0777	0.1092	0.7112	1.4066	1.9776	-0.1222	-0.0315	-0.5710
CH ₃ CHO	C ₁	NPA	0.8178	-0.2416	0.1317	-0.0389	-3.3849	2.3422	-0.6919	1.0594	0.1706	3.0341
		HPA	0.2998	0.1642	0.0714	0.0391	1.8258	1.0268	0.5624	0.1356	0.0323	0.4644
	O	NPA	0.0072	0.9320	0.0012	0.1501	0.0077	0.0206	2.6692	-0.9248	-0.1489	-2.6486
		HPA	0.2708	0.3782	0.0645	0.0900	0.7160	0.9275	1.2953	-0.1074	-0.0256	-0.3678
CH ₃ COCH ₃	C ₁	NPA	0.3142	-0.2916	0.0500	-0.0464	-1.0775	0.7641	-0.7092	0.6058	0.0963	1.4733
		HPA	0.2108	0.1154	0.0493	0.0270	1.8267	0.5902	0.3231	0.0954	0.0223	0.2671
	O	NPA	-0.2540	0.9286	-0.0404	0.1476	-0.2735	-0.6177	2.2584	-1.1826	-0.1880	-2.8761
		HPA	0.2359	0.3499	0.0552	0.0819	0.6742	0.6605	0.9797	-0.1140	-0.0267	-0.3192
C ₂ H ₅ COC ₂ H ₅	C ₁	NPA	0.3064	-0.2944	0.0487	-0.0468	-1.0408	0.7010	-0.6736	0.6008	0.0955	1.3746
		HPA	0.1346	0.0990	0.0314	0.0231	1.3596	0.3547	0.2609	0.0356	0.0083	0.0938
	O	NPA	-0.2650	0.8751	-0.0421	0.1391	-0.3028	-0.6063	2.0022	-1.1401	-0.1813	-2.6085
		HPA	0.1449	0.2873	0.0338	0.0669	0.5044	0.3818	0.7570	-0.1424	-0.0332	-0.3752
CH ₂ =CHCHO	C ₆	NPA	0.2789	0.2070	0.0558	0.0414	1.3473	1.3401	0.9946	0.0719	0.0144	0.3455
		HPA	0.2062	0.1253	0.0668	0.0406	1.6457	1.2997	0.7898	0.0809	0.0262	0.5099
	C ₁	NPA	0.4355	-0.2288	0.0871	-0.0458	-1.9034	2.0926	-1.0994	0.6643	0.1329	3.1920
		HPA	0.1780	0.1357	0.0577	0.0440	1.3117	1.1219	0.8553	0.0423	0.0137	0.2666
	O	NPA	-0.0560	0.9265	-0.0112	0.1853	-0.0604	-0.2691	4.4518	-0.9825	-0.1965	-4.7209
		HPA	0.1797	0.3414	0.0582	0.1106	0.5264	1.1326	2.1518	-0.1617	-0.0524	-1.0192
CH ₃ CH=CHCHO	C ₆	NPA	0.3437	0.0926	0.0677	0.0182	3.7117	1.4494	0.3905	0.2511	0.0495	1.0589
		HPA	0.1592	0.1114	0.0500	0.0350	1.4291	0.8532	0.5970	0.0478	0.0150	0.2562
	C ₁	NPA	0.4408	-0.2365	0.0868	-0.0466	-1.8638	1.8589	-0.9973	0.6773	0.1334	2.8562
		HPA	0.1741	0.1095	0.0547	0.0344	1.5900	0.9330	0.5868	0.0646	0.0203	0.3462
	O	NPA	-0.0670	0.9281	-0.0132	0.1828	-0.0722	-0.2825	3.9138	-0.9951	-0.1960	-4.1963
		HPA	0.1739	0.2450	0.0546	0.0769	0.7098	0.9319	1.3130	-0.0711	-0.0223	-0.3810
NH ₂ OH	N	NPA	0.1870	0.4140	0.0241	0.0534	0.4517	0.3052	0.6756	-0.2270	-0.0293	-0.3705
		HPA	0.1837	0.9327	0.0276	0.1399	0.1970	0.1738	0.8823	-0.7490	-0.1124	-0.7086
	O	NPA	0.2390	0.2300	0.0308	0.0297	1.0391	0.3900	0.3754	0.0090	0.0012	0.0147
		HPA	-0.0770	0.5114	-0.0116	0.0767	-0.1506	-0.0728	0.4838	-0.5884	-0.0883	-0.5566
CH ₃ ONH ₂	C	NPA	0.0870	0.0680	0.0120	0.0094	1.2794	0.1675	0.1309	0.0190	0.0026	0.0366
		HPA	0.5410	0.0819	0.0801	0.0121	6.6056	0.4409	0.0667	0.4591	0.0679	0.3742
	N	NPA	0.1500	0.3510	0.0207	0.0484	0.4274	0.2888	0.6757	-0.2010	-0.0277	-0.3869
		HPA	-0.1510	0.2534	-0.0223	0.0375	-0.5959	-0.1231	0.2065	-0.4044	-0.0599	-0.3296
	O	NPA	0.0720	0.1740	0.0099	0.0240	0.4138	0.1386	0.3350	-0.1020	-0.0141	-0.1964
		HPA	-0.1790	0.9011	-0.0265	0.1334	-0.1986	-0.1459	0.7344	-1.0801	-0.1599	-0.8803
CH ₃ NHOH	C	NPA	0.0470	0.0740	0.0068	0.0107	0.6351	0.0776	0.1222	-0.0270	-0.0039	-0.0446
		HPA	0.4598	0.1677	0.0736	0.0268	2.7418	0.3830	0.1397	0.2921	0.0467	0.2433
	N	NPA	0.1200	0.3390	0.0173	0.0488	0.3540	0.1982	0.5600	-0.2190	-0.0315	-0.3618
		HPA	-0.0580	0.7950	-0.0093	0.1272	-0.0730	-0.0483	0.6622	-0.8530	-0.1365	-0.7105
	O	NPA	0.2100	0.1770	0.0302	0.0255	1.1864	0.3469	0.2924	0.0330	0.0048	0.0545
		HPA	-0.2690	0.4537	-0.0430	0.0726	-0.5929	-0.2241	0.3779	-0.7227	-0.1156	-0.6020
OHCH ₂ CH ₂ NH ₂	C ₁	NPA	0.0540	0.0330	0.0081	0.0050	1.6364	0.0994	0.0607	0.0210	0.0032	0.0386
		HPA	0.1186	0.0254	0.0190	0.0041	4.6693	0.0856	0.0183	0.0932	0.0149	0.0673
	C ₂	NPA	0.0400	0.0610	0.0060	0.0092	0.6557	0.0736	0.1122	-0.0210	-0.0032	-0.0386
		HPA	0.4003	0.1067	0.0640	0.0171	3.7516	0.2890	0.0770	0.2936	0.0470	0.2120
	N	NPA	0.0630	0.3470	0.0095	0.0521	0.1816	0.1159	0.6385	-0.2840	-0.0426	-0.5226
		HPA	-0.3040	0.9520	-0.0486	0.1523	-0.3193	-0.2195	0.6873	-1.2560	-0.2010	-0.9068
	O	NPA	0.1400	0.1010	0.0210	0.0152	1.3861	0.2576	0.1858	0.0390	0.0059	0.0718
		HPA	-0.3340	0.5965	-0.0534	0.0954	-0.5599	-0.2411	0.4307	-0.9305	-0.1489	-0.6718
CH ₃ SNH ₂	C	NPA	0.0550	0.0640	0.0090	0.0105	0.8594	0.1000	0.1164	-0.0090	-0.0015	-0.0164
		HPA	0.0667	0.3358	0.0147	0.0742	0.1986	0.0978	0.4923	-0.2691	-0.0595	-0.3945
	N	NPA	0.1490	0.0820	0.0244	0.0134	1.8171	0.2710	0.1492	0.0670	0.0110	0.1219
		HPA	-0.2970	0.4790	-0.0656	0.1059	-0.6200	-0.4354	0.7022	-0.7760	-0.1715	-1.1376
	S	NPA	0.3580	0.5510	0.0587	0.0904	0.6497	0.6512	1.0023	-0.1930	-0.0317	-0.3511
		HPA	0.3671	0.6485	0.0811	0.1433	0.5661	0.5382	0.9507	-0.2814	-0.0622	-0.4125
CH ₃ NHSH	C	NPA	0.0530	0.0540	0.0084	0.0086	0.9815	0.1109	0.1130	-0.0010	-0.0002	-0.0021
		HPA	0.1715	0.1732	0.0367	0.0371	0.9902	0.3307	0.3339	-0.0017	-0.0004	-0.0033
	N	NPA	0.1310	0.1740	0.0208	0.0277	0.7529	0.2741	0.3640	-0.0430	-0.0068	-0.0900
		HPA	-0.2250	0.9064	-0.0482	0.1940	-0.2482	-0.4338	1.7475	-1.1314	-0.2421	-2.1813
	S	NPA	0.4530	0.4420	0.0720	0.0703	1.0249	0.9477	0.9247	0.0110	0.0017	0.0230
		HPA	0.3479	0.2249	0.0745	0.0481	1.5469	0.6708	0.4336	0.1230	0.0263	0.2371
SHCH ₂ CH ₂ NH ₂	C ₁	NPA	0.0780	0.0410	0.0124	0.0065	1.9024	0.1452	0.0763	0.0370	0.0059	0.0689
		HPA	0.0117	0.2268	0.0024	0.0458	0.0516	0.0158	0.3064	-0.2151	-0.0435	-0.2906
	C ₂	NPA	0.0290	0.0250	0.0046	0.0040	1.1600	0.0540	0.0466	0.0040	0.0006	0.0074
		HPA	0.1651	0.0876	0.0334	0.0177	1.8847	0.2231	0.1183	0.0775	0.0157	0.1047
	N	NPA	0.0380	0.1270	0.0060	0.0202	0.2992	0.0708	0.2365	-0.0890	-0.0142	-0.1657
		HPA	-0.2920	0.7628	-0.0590	0.1541	-0.3828	-0.3945	1.0305	-1.0548	-0.2131	-1.4250
	S	NPA	0.3890	0.4710	0.0619	0.0749	0.8259	0.7243	0.8770	-0.0820	-0.0130	-0.1527
		HPA	0.1064	0.5646	0.0215	0.1140	0.1885	0.1437	0.7628	-0.4582	-0.0926	-0.6190

of multiphlic descriptor $\Delta\omega(r)$ is that it provides a higher value in terms of magnitude compared to other dual descriptors. For instance, values of Δf_k , Δs_k , and $\Delta\omega_k$ for nucleophilic (electrophilic) attack at the carbonyl carbon (oxygen) site of $\text{CH}_3\text{-CHO}$ are 1.06 (−0.93), 0.17 (−0.15), 3.03 (−2.65), respectively, for NPA-derived charges. Almost the same trend is followed in the case of HPA-derived charges.

The second group of compounds, namely, α -, β -conjugated carbonyl, are elaborately studied in the recent past because of the presence of two reactive centers.³⁵ The first reactive site is the carbon (C_1) of the carbonyl, and the second is the carbon in the β position (C_6). In such a case, the β carbon is activated because of the withdrawing mesomeric effect of the adjacent carbonyl group. As seen from Table 2, NPA-derived charges give a maximum value for f_k^+ to the carbonyl carbon, whereas HPA-derived charges provide the maximum f_k^+ value to the β carbon atom (C_6) in the case of the $\text{CH}_2=\text{CHCHO}$ molecule. For $\text{CH}_3\text{CH}=\text{CHCHO}$, NPA (HPA) provide a maximum f_k^+ value of 0.44 (0.17) to the carbonyl carbon (C_1) compared to the β carbon site of 0.34 (0.16). This ambiguous behavior may be due to the dependence of local reactivity descriptors on the selection of the basis set and population schemes.³⁴ Further oxygen site shows a high value for f_k^+ and other local descriptors, making it difficult to predict the proper electrophilic site. Even now $\Delta\omega_k$ exhibits high positive value on both carbons that are supposed to be electrophilic and a high negative value on the oxygen site disclosing clearly its nucleophilic character compared to other dual descriptors. Also it can be noted from Table 2 that, even for molecules with more than one reactive site, $\Delta\omega_k$ is capable of making a clear distinction among them in terms of their magnitude. That is, for molecules 5 and 6 having two reactive sites as the carbon (C_1) of the carbonyl and the carbon in the β position (C_6), our descriptors are capable of distinctly identifying the stronger site (electrophilic/nucleophilic).

Optimized structures along with atom numbering for the selected set of amines are presented in Supporting Information Figure S2. Global and local reactivity properties of the selected set of amines calculated using B3LYP/6-311+G** and BLYP/DND methods are presented in Tables 1 and 2, respectively. Global reactivity trend based on ω (toward a nucleophile) is given by the following.

B3LYP/6-311+G** method (Table 1):

- (i) $\text{CH}_3\text{ONH}_2 > \text{OHCH}_2\text{CH}_2\text{NH}_2 > \text{CH}_3\text{NHOH} > \text{NH}_2\text{OH}$.
- (ii) $\text{CH}_3\text{NHSH} > \text{SHCH}_2\text{CH}_2\text{NH}_2 > \text{CH}_3\text{SNH}_2$.

BLYP/DND method (Table 1):

- (i) $\text{NH}_2\text{OH} > \text{CH}_3\text{NHOH} > \text{CH}_3\text{ONH}_2 > \text{OHCH}_2\text{CH}_2\text{NH}_2$.
- (ii) $\text{CH}_3\text{NHSH} > \text{CH}_3\text{SNH}_2 > \text{SHCH}_2\text{CH}_2\text{NH}_2$.

Variations in the qualitative trends in the above two sets appear to stem from the different energy functionals and basis sets used.

On the basis of the NPA and HPA charge-derived multiphlic descriptor at the nitrogen site ($\Delta\omega_N$), the following reactivity trend (toward a nucleophile) has been obtained.

NPA (Table 2):

- (1) $\text{OHCH}_2\text{CH}_2\text{NH}_2 > \text{CH}_3\text{ONH}_2 > \text{NH}_2\text{OH} > \text{CH}_3\text{NHOH}$.
- (2) $\text{SHCH}_2\text{CH}_2\text{NH}_2 > \text{CH}_3\text{NHSH} > \text{CH}_3\text{SNH}_2$.

HPA (Table 2):

- (1) $\text{OHCH}_2\text{CH}_2\text{NH}_2 > \text{CH}_3\text{NHOH} > \text{NH}_2\text{OH} > \text{CH}_3\text{ONH}_2$.
- (2) $\text{CH}_3\text{NHSH} > \text{SHCH}_2\text{CH}_2\text{NH}_2 > \text{CH}_3\text{SNH}_2$.

So far as the intramolecular reactivity trends are concerned, the site with maximum negative value of $\Delta\omega_k$ is the most preferred site for electrophilic attack. Chemical intuition suggests that the N site is more prone toward electrophilic attack. Table

TABLE 3: Atomic Site with Maximum Value for Multiphlic Descriptor ($\Delta\omega_k$) for the Selected Set of Amines

molecule	site with maximum value for $\Delta\omega_k$	
	NPA	HPA
NH_2OH	N	N
CH_3ONH_2	N	O
CH_3NHOH	N	N
$\text{OHCH}_2\text{CH}_2\text{NH}_2$	N	N
CH_3SNH_2	S	N
CH_3NHSH	N	N
$\text{SHCH}_2\text{CH}_2\text{NH}_2$	N	N

TABLE 4: Global Reactivity Descriptors Calculated at the B3LYP/6-31G* Level of Theory

species	η (eV)	μ (eV)	ω (eV)
reactant	3.64	−2.89	1.15
transition state	2.48	−2.79	1.57
product	3.64	−2.89	1.15

TABLE 5: Global Reactivity Descriptors along the Intrinsic Reaction Coordinate Calculated at the B3LYP/6-31G* Level of Theory

points along IRC	E (hartrees) ^a	η (eV)	μ (eV) ^a	ω (eV)	α (au)
1	−234.5673	2.65	−2.7825	1.46	64.94
2	−234.5661	2.63	−2.7827	1.47	65.21
3	−234.5649	2.61	−2.7828	1.49	65.47
4	−234.5638	2.59	−2.7836	1.50	65.74
5	−234.5628	2.57	−2.7836	1.51	65.98
6	−234.5618	2.55	−2.7843	1.52	66.22
7	−234.5608	2.54	−2.7843	1.53	66.42
8	−234.5600	2.53	−2.7851	1.54	66.63
9	−234.5592	2.51	−2.7852	1.54	66.80
10	−234.5586	2.50	−2.7859	1.55	66.96
11	−234.5580	2.50	−2.7857	1.56	67.07
12	−234.5576	2.49	−2.7866	1.56	67.20
13	−234.5576	2.49	−2.7866	1.56	67.20
14	−234.5580	2.50	−2.7857	1.56	67.07
15	−234.5586	2.50	−2.7859	1.55	66.96
16	−234.5592	2.51	−2.7852	1.54	66.80
17	−234.5600	2.53	−2.7851	1.54	66.63
18	−234.5608	2.54	−2.7843	1.53	66.42
19	−234.5618	2.55	−2.7843	1.52	66.22
20	−234.5628	2.57	−2.7836	1.51	65.98
21	−234.5638	2.59	−2.7836	1.50	65.74
22	−234.5649	2.61	−2.7830	1.49	65.47
23	−234.5661	2.63	−2.7827	1.47	65.21
24	−234.5673	2.65	−2.7825	1.46	64.94

^a For these columns up to four decimal results are provided.

3 lists the site with the maximum negative value for $\Delta\omega_k$ for the selected set of amines. It is seen that with a few exceptions, the N site is predicted as the most preferred site for electrophilic attack.

Further, in order to test $\Delta\omega_k$ along the intrinsic reaction coordinate (IRC), we consider a cope rearrangement of hexa-1,5-diene. This is an example of a [3,3] sigmatropic reaction. Supporting Information Figure S3 provides the optimized geometrical structures with atom numbering for the reactant, transition state, and product calculated using the B3LYP/6-31G* level of theory. Table 4 gives the global reactivity parameters of the reactant, transition state, and product. As expected, hardness is minimum (2.48 eV) and the corresponding electrophilicity index is maximum (1.57 eV) at the transition state. Variation of the global reactivity parameter along the IRC path is presented in Table 5 and Figure 1, parts a and b. Variation of energy (E) and ω along the IRC path is given in Figure 1a. It is seen that both E and ω are maximum around the transition

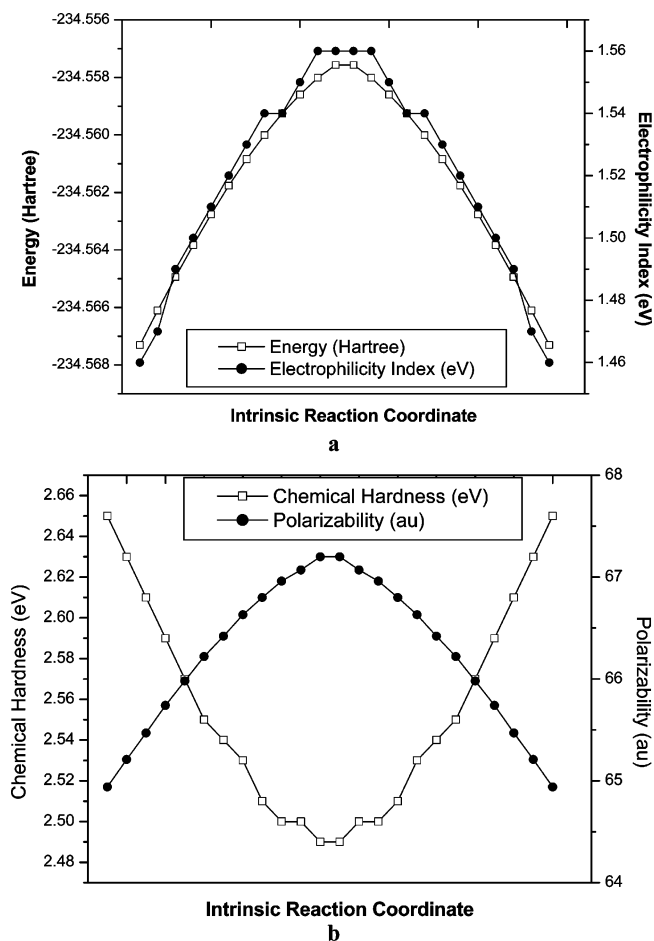


Figure 1. (a and b) Variation of global reactivity descriptors along the intrinsic reaction coordinate (IRC).

state indicating it as the most unstable structure along the IRC path. Figure 1b provides the variation of hardness (η) and polarizability (α) along the IRC path. An inverse relationship exists between them. That is, η reaches a minimum, whereas α becomes maximum at the transition state as expected.

Variation of the multiphilic descriptor ($\Delta\omega_k$) along the IRC for the important atomic sites (C_1 , and C_3/C_6 , and C_{11}) is presented in Figure 2. In going from reactant to product, C_1 and C_3 (C_6 and C_{11}) sites change their nature and become more prone toward electrophilic attack (nucleophilic attack) at the product side. This change in the nature of attack takes place around the transition state. It is important to note that ω is always positive, whereas Δf_r changes its sign in the neighborhood of the transition state confirming our prognosis that the former takes care of the electron transfer and the latter decides the direction of the same. The interplay of variation of these global and local descriptors along the IRC provides the characteristic step-function-like look.

In studying the importance of nucleophilicity excess ($\Delta\omega_g^\mp$) descriptor, a careful analysis on the electronic structure, property, and reactivity of all-metal aromatic compounds, viz., MAI_4^- ($M = Li, Na, K, \text{ and } Cu$) is performed. The four-membered aluminum unit Al_4 present in all the molecules may be considered as a single unit. This unit can easily take part in the charge-transfer process with the M ($\equiv Li, Na, K, Cu$) atom in those complexes.

Figure 3 shows the various stable isomers of MAI_4^- . The C_{4v} isomer of the MAI_4^- is reported as the energetically most stable, least polarizable, and hardest.^{36,37} Table 6 presents the group philicity (ω_g^+ , ω_g^-) values of the Al_4^{2-} nucleophile and

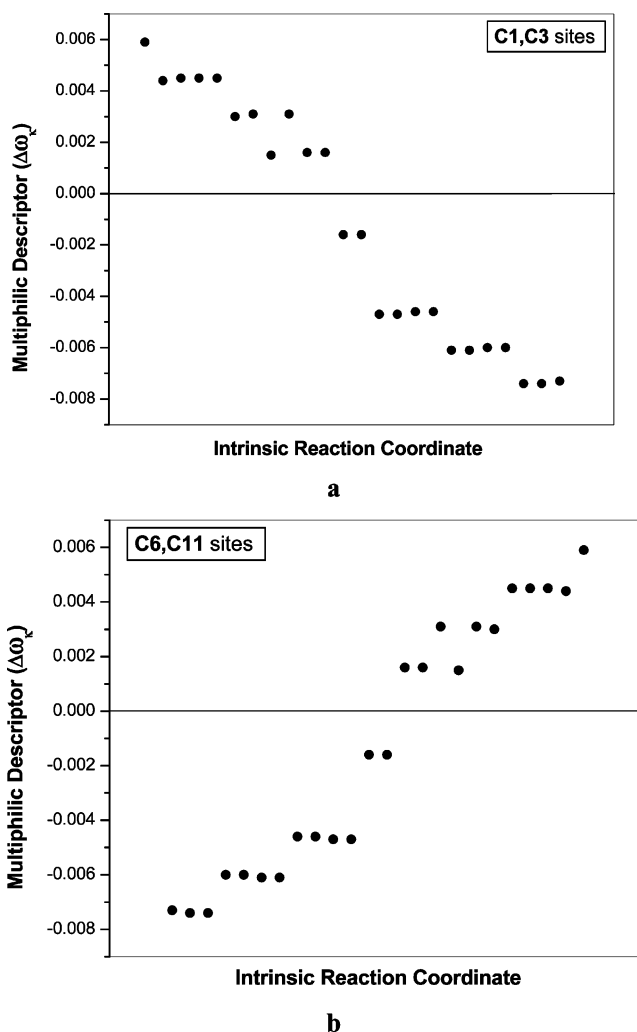
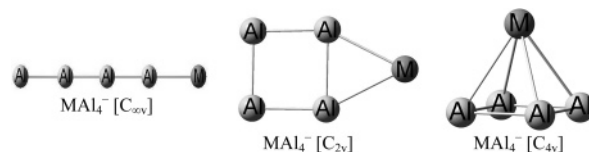


Figure 2. (a and b) Variation of multiphilic descriptor along the intrinsic reaction coordinate (IRC) for the selected atomic sites.



$M = Li, Na, K, Cu$

Figure 3. Stable structures of various isomers of MAI_4^- ($M \equiv Li, Na, K, Cu$).

M^+ ($M = Li, Na, K, Cu$) electrophile in the MAI_4^- isomers. It is found that in all MAI_4^- isomers the nucleophilicity of the Al_4^{2-} aromatic unit overwhelms its electrophilic trend (i.e., $\omega_g^- > \omega_g^+$), and therefore $\Delta\omega_g^\mp$ is positive, whereas the electrophilicity of M^+ dominates over its nucleophilicity (i.e., $\omega_g^+ > \omega_g^-$), and therefore $\Delta\omega_g^\mp$ is negative as expected. It is important to note that $\Delta\omega_g^\mp$ of Al_4^{2-} is maximum in the case of the most stable C_{4v} isomer of the MAI_4^- molecule. The order of the $\Delta\omega_g^\mp$ value of the Al_4^{2-} nucleophile in MAI_4^- , $C_{4v} > C_{2v} > C_{\infty v}$, i.e., stabilization of an MAI_4^- isomer (except in KAl_4^-) increases the nucleophilicity of the associated Al_4^{2-} unit and accordingly can be used as a better molecular cathode. It is also important to note that the nucleophilicity of the Al_4^{2-} unit in MAI_4^- (C_{4v}) increases as $K < Cu < Na < Li$ according to the respective nucleophilicity excess values. Standard expressions¹⁻⁵

TABLE 6: Group Philicity (ω_g^+ , ω_g^-) Values for Nucleophilic and Electrophilic Attacks, Respectively, for the Ionic Units of Different Isomers of LiAl_4^- , NaAl_4^- , KAl_4^- , and CuAl_4^-

isomers	ionic unit	ω_g^+	ω_g^-	$\Delta\omega_g^\ddagger$
LiAl_4^- ($C_{\infty v}$)	Al_4^{2-} Li^+	0.0070 0.0063	0.0095 0.0037	0.0025 -0.0025
LiAl_4^- (C_{2v})	Al_4^{2-} Li^+	1.3×10^{-5} 0.0068	0.0055 0.0013	0.0055 -0.0055
LiAl_4^- (C_{4v})	Al_4^{2-} Li^+	-0.0372 0.4055	0.2965 0.0718	0.3338 -0.3338
NaAl_4^- ($C_{\infty v}$)	Al_4^{2-} Na^+	0.0070 0.0074	0.0102 0.0042	0.0032 -0.0032
NaAl_4^- (C_{2v})	Al_4^{2-} Na^+	-0.0001 0.0096	0.0078 0.0017	0.0079 -0.0079
NaAl_4^- (C_{4v})	Al_4^{2-} Na^+	-0.0073 0.1301	0.1024 0.0204	0.1097 -0.1097
KAl_4^- ($C_{\infty v}$)	Al_4^{2-} K^+	0.0044 0.0106	0.0095 0.0054	0.0051 -0.0051
KAl_4^- (C_{2v})	Al_4^{2-} K^+	0.0023 0.0118	0.0101 0.0039	0.0078 -0.0078
KAl_4^- (C_{4v})	Al_4^{2-} K^+	0.0008 0.0078	0.0066 0.0021	0.0057 -0.0057
CuAl_4^- ($C_{\infty v}$)	Al_4^{2-} Cu^+	0.0031 0.0014	0.0036 0.0009	0.0006 -0.0006
CuAl_4^- (C_{2v})	Al_4^{2-} Cu^+	0.0036 0.0008	0.0036 0.0008	0.0048 -0.0048
CuAl_4^- (C_{4v})	Al_4^{2-} Cu^+	0.0178 0.0131	0.0332 -0.0023	0.0154 -0.0154

for ΔN and ΔE in terms of group electronegativity and group hardness will provide additional insights into the electron-transfer process.

Variation of $\Delta\omega_k$ along the IRC of three selected reactions,³⁸ viz., (a) a thermoneutral reaction, $\text{F}_a^- + \text{CH}_3-\text{F}_b \rightarrow \text{F}_a-\text{CH}_3 + \text{F}_b^-$, (b) an endothermic reaction, $\text{HNO} \rightarrow \text{HON}$, and (c) an exothermic reaction, $\text{H}_2\text{OO} \rightarrow \text{HOOH}$, is provided in Figure 4a–c. For the thermoneutral reaction, both the F_a^- (bond making) and F_b^- (bond breaking) are nucleophilic. The net nucleophilicity of the F_a^- atom is more than that of the F_b^- atom along the IRC from reactant side to TS, and the situation is reversed for the IRCs pertaining to the TS to product side. For the endothermic reaction, the net nucleophilicity of O (bond making) is higher than that of N (bond breaking) along the IRC. In the case of exothermic reaction, the O1 (bond making) atom is more electrophilic than its nucleophilic activity. Considering the problems associated with HPA which are absent in the Mulliken population analysis (MPA) scheme,³⁴ the FF values are calculated using the MPA scheme, which become negative in some cases. For the thermoneutral reaction $\Delta\omega_k$ is minimum at the transition state. For the other two reactions, $\Delta\omega_k$ does not always follow the trend that the IRC corresponding to the minimum value of ω_k^\ddagger (if not zero) is in accordance with the Hammond's postulate.³⁷ Figure 5a–c provides the profiles for the corresponding reaction forces.³⁹

Apart from the important points corresponding to the reactant (R), the transition state (TS) and the product (P) there exists two other important points associated with the configurations having the force maximum (F_{max}) and the force minimum (F_{min}).³⁹ The zeroes, maxima, and minima of the reaction force define key points along the reaction coordinate, which divide it into three reaction regions that are identified through vertical dashed lines in Figure 5. The first stage, in the reactant region, tends to be preparative in nature with emphasis in structural effects, such as rotation, bond stretching, angle bending, etc., that will facilitate subsequent steps. The transition state region is mostly characterized by electronic rearrangements, whereas

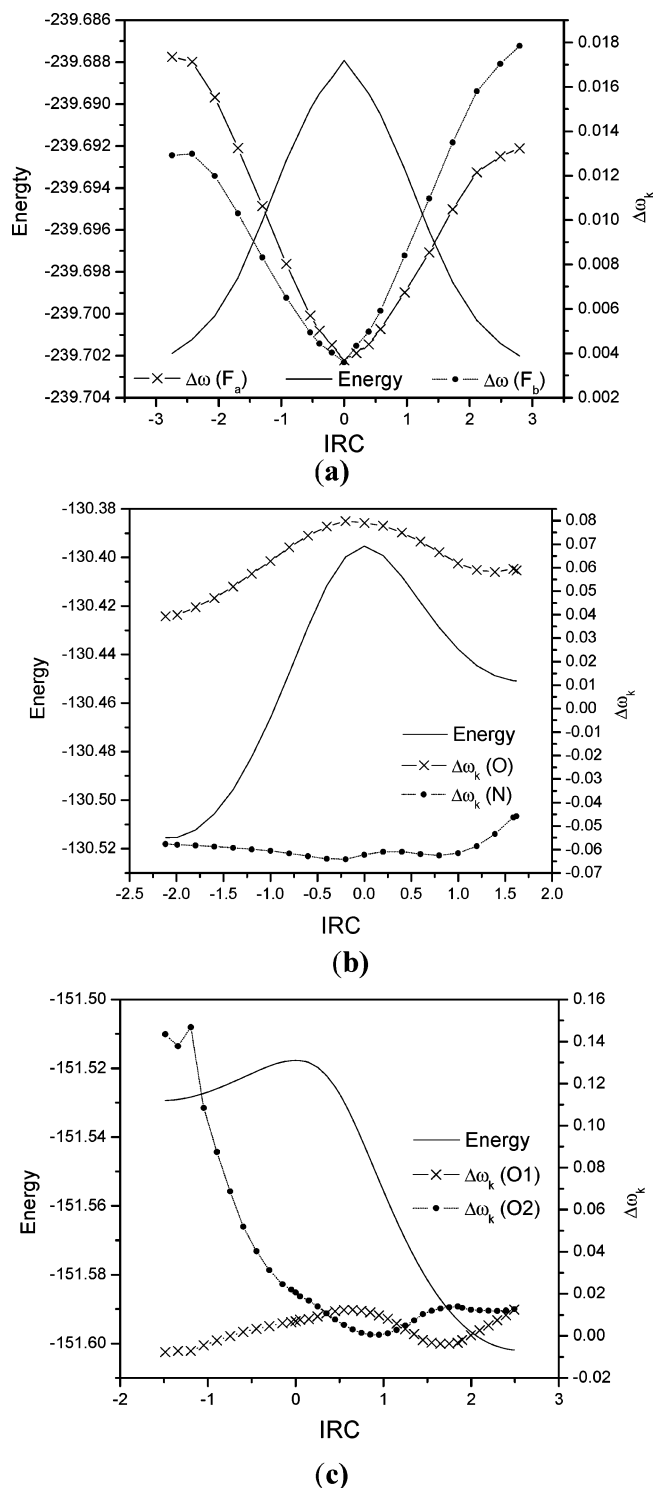


Figure 4. (a–c) Profiles of net nucleophilicity ($\Delta\omega_k$) of along the path of the gas phase: (a) thermoneutral $\text{S}_{\text{N}}2$ substitution, $\text{F}_a^- + \text{CH}_3-\text{F}_b \rightarrow \text{F}_a-\text{CH}_3 + \text{F}_b^-$; (b) endothermic reaction, $\text{HNO} \rightarrow \text{HON}$; (c) exothermic reaction, $\text{H}_2\text{OO} \rightarrow \text{HOOH}$. Also shown is the profile of energy.

the product region is mainly associated to structural relaxation necessary to reach the products. We have shown that analyzing a chemical reaction in terms of these regions can provide significant insight into its mechanism and the roles played by external factors, such as external potentials and solvents.^{39,40} Partition of the activation energies in terms of the work done in going from (i) R to F_{min} , W_1 ; (ii) F_{min} to TS, W_2 ; (iii) TS to F_{max} , W_3 ; (iv) F_{max} to P, W_4 gives the activation energy for the forward reaction (E_f^\ddagger) as ($W_1 + W_2$) and that of the reverse

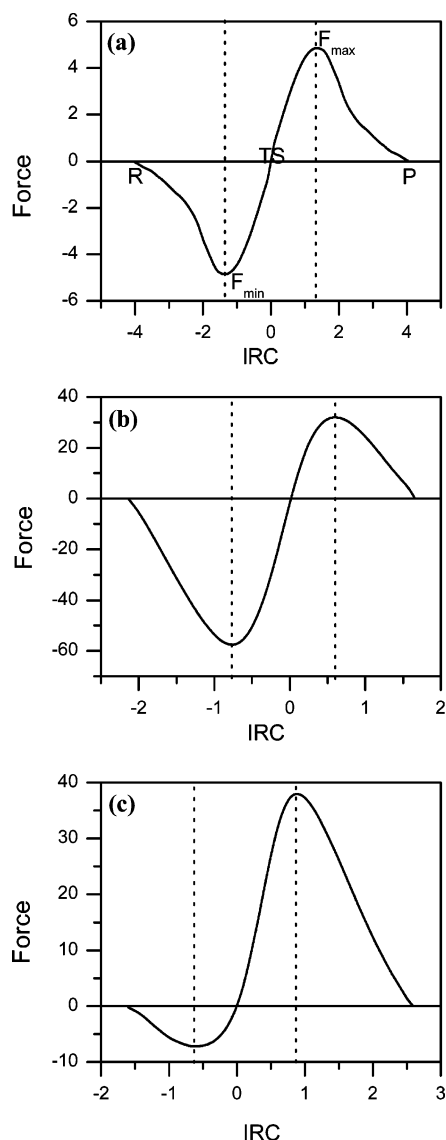


Figure 5. Reaction force profiles along the reaction coordinate for (a) thermoneutral reaction, $F_a^- + CH_3-F_b \rightarrow F_a^-CH_3 + F_b^-$; (b) endothermic reaction, $HNO \rightarrow HON$; (c) the exothermic reaction, $H_2OO \rightarrow HOOH$. The vertical dashed lines define the reaction regions as follows: reactant (left), transition state (middle), and product (right).

reaction (E_r^\ddagger) as $-(W_3 + W_4)$. Therefore, the reaction energy (ΔE^0) becomes ($E_r^\ddagger - E_r^\ddagger = W_1 + W_2 + W_3 + W_4$). These values are provided in Table 7. As expected ΔE^0 is zero, negative, and positive for the thermoneutral, exothermic, and endothermic reactions, respectively. The skew-symmetric nature of the force profile for the thermoneutral reaction suggests that $A = W_1 + W_4$ and $B = W_2 + W_3$ would be zero. Similarly A , B would be positive (negative) for the endo(exo)thermic reactions. The transition state at the IRC = 0 configuration lies

at the middle between the F_{max} and F_{min} configurations for the thermoneutral reaction, whereas it lies toward the F_{min} (F_{max}) configurations for the exo(endo)thermic reaction, a signature of the Hammond postulate via reaction force.

Similar values of W_1 and W_2 (see Table 7) together with the changes observed in the nucleophilicity along the reaction coordinate for the thermoneutral S_N2 substitution and for the exothermic reaction $H_2OO \rightarrow HOOH$ indicate that structural and electronic reordering show up at the very beginning of the reaction,^{39,40} through a sharp decrease of the nucleophilicity; this change practically ceases at the transition state of the exothermic reaction to reach the product value. It is interesting to note that in both cases the lowering of nucleophilicity of the key atoms from the reactants ($\Delta\omega(F_a/F_b) \sim 0.014$; $\Delta\omega(O1) \sim 0.14$) to the transition state ($\Delta\omega(F_a/F_b) \sim 0.004$; $\Delta\omega(O1) \sim 0.0$) requires a similar amount of energy (9.54 kcal/mol and 7.39 kcal/mol, respectively). It can be observed in Table 7 that for the thermoneutral reaction $W_1 > W_2$ indicating that the preparation step requires more energy than the transition to product step. On the other hand, the W_2 values for the thermoneutral and exothermic reactions are quite close to each other and the work W_1 associated to the preparation step in the thermoneutral reaction is larger than that of the exothermic reaction; this indicates that in the S_N2 reaction the structural reordering of the CH_3 group to reach the D_{3h} structure at the transition state is the key transformation that involves most of the activation energy. In the endothermic $HNO \rightarrow HON$ reaction the small changes of nucleophilicity together with large values of W_1 and W_2 indicate that the reaction is mainly driven by the structural reordering in the preparation step.

5. Conclusions

A multiphlicity descriptor ($\Delta\omega_k$) is proposed and tested in this work. It is shown that $\Delta\omega_k$ helps in identifying the electrophilic/nucleophilic nature of a specific site within a molecule. A comparison between different local reactivity descriptors is carried out on a set of carbonyl compounds. Also a selected set of amines is analyzed using $\Delta\omega_k$. Further, we also consider a cope rearrangement of hexa-1,5-diene to test the variation of $\Delta\omega_k$ along the IRC path. It is seen that $\Delta\omega_k$ presents a clear distinction between electrophilic and nucleophilic sites within a molecule in terms of their magnitude and sign. Hence, they reveal the fact that multiphlicity descriptor can effectively be used in characterizing the electrophilic/nucleophilic nature of a given site in a molecule. Also, the importance of nucleophilicity excess ($\Delta\omega_g^\mp$) descriptor on the reactivity of all-metal aromatic compounds, viz., MAI_4^- ($M = Li, Na, K,$ and Cu), is successfully analyzed. Important insights into three different types of reactions, viz. (a) thermoneutral, (b) endothermic, and (c) exothermic, are obtained through the analysis of the multiphlicity descriptor profiles within the reaction regions defined by the reaction force along the reaction path.

The results discussed so far clearly show the importance of the selected descriptors, namely, the multiphlicity descriptor and

TABLE 7: Profiles of the Forward Activation Energy (ΔE_f^\ddagger), Reverse Activation Energy (ΔE_r^\ddagger), and Reaction Energy (ΔE^0) of a Thermoneutral Reaction ($F_a^- + CH_3-F_b \rightarrow F_a^-CH_3 + F_b^-$), an Endothermic Reaction ($HNO \rightarrow HON$), and an Exothermic Reaction ($H_2OO \rightarrow HOOH$)

reaction	ΔE_f^\ddagger	ΔE_r^\ddagger	ΔE^0	ξ_1	ξ_2	W_1	W_2	W_3	W_4
thermoneutral B3LYP/6-311++G**	9.54	9.54	0.0	-1.33	1.33	5.42	4.12	-4.12	-5.42
endothermic B3LYP/6-311++G**	75.39	34.84	40.55	-0.80	0.60	43.97	31.42	-13.20	-21.64
exothermic B3LYP/6-311++G**	7.39	52.85	-45.46	-0.65	0.87	3.93	3.46	-19.99	-32.86

nucleophilicity excess, in analyzing the overall reactivity trends in molecular systems.

Acknowledgment. P.K.C. and D.R.R. thank BRNS, Mumbai for financial assistance. P.K.C. and A.T.L. also thank P. W. Ayers for helpful discussions. J.P. and B.S.K. thank the IIT Kharagpur for providing the facilities required for a summer project. J.P. also thanks the UGC for selecting him to carry out his Ph.D. work under FIP. A.T.-L. and S.G.-O. wish to express thanks for the financial support from FONDECYT, Grant No. 1060590, FONDAP through Project No. 11980002 (CIMAT), and Programa Bicentenario en Ciencia y Tecnología (PBCT), Proyecto de Inserción Académica No. 8. A.T.-L. is also indebted to the John Simon Guggenheim Foundation for a sabbatical fellowship.

Supporting Information Available: Figures of optimized structures. This material is available free of charge via the Internet at <http://pubs.acs.org>.

Note Added after ASAP Publication. The incorrect version of this article was released ASAP on August 23, 2007. The correct version, which includes an additional sentence in the text following equation 5 and revised reference 8 was posted on August 24, 2007.

References and Notes

- Parr, R. G.; Yang, W. *Density Functional Theory of Atoms and Molecules*; Oxford University Press: Oxford, 1989.
- Pearson, R. G. *Chemical Hardness—Applications from Molecules to Solids*; VCH-Wiley: Weinheim, Germany, 1997.
- Geerlings, P.; De Proft, F.; Langenaeker, W. *Chem. Rev.* **2003**, *103*, 1793.
- Chattaraj, P. K., Ed. *J. Chem. Sci.* **2005**, *117*, 367–615, special issue on chemical reactivity.
- (a) Parr, R. G.; Szentpaly, L. V.; Liu, S. *J. Am. Chem. Soc.* **1999**, *121*, 1922. (b) Chattaraj, P. K.; Sarkar, U.; Roy, D. R. *Chem. Rev.* **2006**, *106*, 2065.
- (a) Parr, R. G.; Yang, W. *J. Am. Chem. Soc.*, **1984**, *106*, 4049. (b) Fukui, K. *Science* **1987**, *218*, 747. (c) Ayers, P. W.; Levy, M. *Theor. Chem. Acc.* **2000**, *103*, 353.
- Yang, W.; Mortier, W. J. *J. Am. Chem. Soc.* **1986**, *108*, 5708.
- (a) Chattaraj, P. K.; Maiti, B.; Sarkar, U. *J. Phys. Chem. A* **2003**, *107*, 4973. (b) Roy, D. R.; Parthasarathi, R.; Padmanabhan, J.; Sarkar, U.; Subramanian, V.; Chattaraj, P. K. *J. Phys. Chem. A* **2006**, *110*, 1084.
- Parthasarathi, R.; Padmanabhan, J.; Subramanian, V.; Maiti, B.; Chattaraj, P. K. *J. Phys. Chem. A* **2003**, *107*, 10346.
- Parthasarathi, R.; Padmanabhan, J.; Subramanian, V.; Maiti, B.; Chattaraj, P. K. *Curr. Sci.* **2004**, *86*, 535.
- Padmanabhan, J.; Parthasarathi, R.; Subramanian, V.; Chattaraj, P. K. *Chem. Res. Toxicol.* **2006**, *19*, 356.
- Yang, W.; Parr, R. G. *Proc. Natl. Acad. Sci. U.S.A.* **1985**, *82*, 6723.
- Lee, C.; Yang, W.; Parr, R. G. *J. Mol. Struct. (THEOCHEM)* **1988**, *163*, 305.
- Roy, R. K.; Krishnamurti, S.; Geerlings, P.; Pal, S. *J. Phys. Chem. A* **1998**, *102*, 3746.
- Langenaeker, W.; De Proft, F.; Geerlings, P. *J. Mol. Struct. (THEOCHEM)* **1996**, *362*, 175.
- De Proft, F.; Martin, M. L. J.; Geerlings, P. *Chem. Phys. Lett.* **1996**, *256*, 400.
- Contreras, R.; Fuentealba, P.; Galván, M.; Pérez, P. *Chem. Phys. Lett.* **1999**, *304*, 405.
- Thanikaivelan, P.; Padmanabhan, J.; Subramanian, V.; Ramasami, T. *Theor. Chem. Acc.* **2002**, *107*, 326.
- Parthasarathi, R.; Padmanabhan, J.; Elango, M.; Subramanian, V.; Chattaraj, P. K. *Chem. Phys. Lett.* **2004**, *394*, 225.
- Morell, C.; Grand, A.; Toro-Labbé, A. *J. Phys. Chem. A* **2005**, *109*, 205.
- Padmanabhan, J.; Parthasarathi, R.; Subramanian, V.; Chattaraj, P. K. *J. Phys. Chem. A* **2006**, *110*, 2739.
- Harbola, M. K.; Chattaraj, P. K.; Parr, R. G. *Isr. J. Chem.* **1991**, *321*, 395.
- Morell, C.; Grand, A.; Toro-Labbe, A. *Chem. Phys. Lett.* **2006**, *425*, 342.
- Chamorro, E.; Chattaraj, P. K.; Fuentealba, P. *J. Phys. Chem. A* **2003**, *107*, 7068.
- (a) Fuentealba, P.; Parr, R. G. *J. Chem. Phys.* **1991**, *94*, 5559. (b) Gutiérrez-Oliva, S.; Jaque, P.; Toro-Labbé, A. *J. Phys. Chem. A* **2000**, *104*, 8955.
- Perdew, J. P.; Parr, R. G.; Levy, M.; Balduz, J. L., Jr. *Phys. Rev. Lett.* **1982**, *49*, 1691.
- Ayers, P. W.; Morell, C.; De Proft, F.; Geerlings, P. 2007, Unpublished work.
- Gaussian 98*, revision A.5; Gaussian Inc.: Pittsburgh, PA, 1998.
- Reed, A. E.; Weinhold, F. *J. Chem. Phys.* **1983**, *78*, 4066.
- Reed, A. E.; Weinstock, R. B.; Weinhold, F. *J. Chem. Phys.* **1985**, *83*, 735.
- Hirshfeld, F. L. *Theor. Chim. Acta* **1977**, *44*, 129.
- DMOL³*; Accelrys, Inc.: San Diego, CA, 2001.
- March, J. *Advanced Organic Chemistry: Reactions, Mechanisms and Structure*; Wiley & Sons: New York, 1998.
- (a) Bulat, F.; Chamorro, E.; Fuentealba, P.; Toro-Labbé, A. *J. Phys. Chem. A* **2004**, *108*, 342. (b) Bultnick, P. *Faraday Discuss.* **2007**, *135*, 244. (c) Bultnick, P.; Carbó-Dorca, R. *J. Phys. Chem. A* **2007**, *111*, 2640.
- (a) Patai, S.; Rappoport, Z. In *The Chemistry of Alkenes*; Patai, S., Ed.; Interscience Publishers: London, 1964; p 469. (b) Wong, S. S.; Paddon-Row, M. N.; Li, Y.; Houk, K. N. *J. Am. Chem. Soc.* **1990**, *112*, 8679. (c) Langenaeker, W.; Demel, K.; Geerlings, P. *J. Mol. Struct. (THEOCHEM)* **1992**, *259*, 317. (d) Dorigo, A. E.; Morokuma, K. *J. Am. Chem. Soc.* **1989**, *111*, 6524.
- (a) Li, X.; Kuznetsov, A. E.; Zhang, H.-F.; Boldyrev, A. I.; Wang, L.-S. *Science* **2001**, *291*, 859. (b) Kuznetsov, A.; Birch, K.; Boldyrev, A. I.; Li, X.; Zhai, H.; Wang, L.-S. *Science* **2003**, *300*, 622.
- (a) Chattaraj, P. K.; Roy, D. R.; Elango, M.; Subramanian, V. *J. Phys. Chem. A* **2005**, *109*, 9590. (b) Roy, D. R.; Chattaraj, P. K.; Subramanian, V. *Indian J. Chem., Sect. A* **2006**, *45A*, 2369. (c) Solà, M.; Toro-Labbé, A. *J. Phys. Chem. A* **1999**, *103*, 8847. (d) Bulat, F. A.; Toro-Labbé, A. *J. Phys. Chem. A* **2003**, *107*, 3987.
- (a) Chattaraj, P. K.; Roy, D. R. *J. Phys. Chem. A* **2006**, *110*, 11401. (b) Chattaraj, P. K.; Roy, D. R. *J. Phys. Chem. A* **2005**, *109*, 3771.
- (a) Toro-Labbé, A. *J. Phys. Chem. A* **1999**, *103*, 4398. (b) Jaque, P.; Toro-Labbé, A. *J. Phys. Chem. A* **2000**, *104*, 995. (c) Martínez, J.; Toro-Labbé, A. *Chem. Phys. Lett.* **2004**, *392*, 132. (d) Herrera, B.; Toro-Labbé, A. *J. Chem. Phys.* **2004**, *121*, 7096. (e) Toro-Labbé, A.; Gutiérrez-Oliva, S.; Concha, M. C.; Murray, J. S.; Politzer, P. *J. Chem. Phys.* **2004**, *121*, 4570. (f) Gutiérrez-Oliva, S.; Herrera, B.; Toro-Labbé, A.; Chermette, H. *J. Phys. Chem. A* **2005**, *109*, 1748.
- (a) Politzer, P.; Burda, J. V.; Concha, M. C.; Lane, P.; Murray, J. S. *J. Phys. Chem. A* **2006**, *110*, 756. (b) Rincón, E.; Jaque, P.; Toro-Labbé, A. *J. Phys. Chem. A* **2006**, *110*, 9478. (c) Burda, J. V.; Toro-Labbé, A.; Gutiérrez-Oliva, S.; Murray, J. S.; Politzer, P. *J. Phys. Chem. A* **2007**, *111*, 2455.